*Journal of Biomolecular NMR*, **19:** 167–179, 2001.
*KLUWER/ESCOM*
© 2001 *Kluwer Academic Publishers. Printed in the Netherlands.*


# 2D relayed anisotropy correlation NMR: Characterization of the $^{13}C'$ chemical shift tensor orientation in the peptide plane of the dipeptide AibAib

Bert Heise[a], Jörg Leppert[a], Holger Wenschuh[b], Oliver Ohlenschläger[a], Matthias Görlach[a] & Ramadurai Ramachandran[a,*]

[a]*Abteilung Molekulare Biophysik/NMR-Spektroskopie, Institut für Molekulare Biotechnologie, Postfach 100813, D-07708 Jena, Germany; and* [b]*Jerini Bio Tools GmbH, Rudower Chaussee 5, D-12489 Berlin, Germany*

Received 28 August 2000; Accepted 13 November 2000

*Key words:* carbonyl chemical shift tensors, MAS, relayed anisotropy correlation, solid state NMR

**Abstract**

An approach to the determination of the orientation of the carbonyl chemical shift (CS) tensor in a $^{13}C'$-$^{15}N$-$^{1}H$ dipolar coupled spin network is proposed. The method involves the measurement of the Euler angles of the $^{13}C'$-$^{15}N$ and $^{15}N$-$^{1}H$ dipolar vectors in the $^{13}C'$ CS tensor principal axes system, respectively, via a $^{13}C$-$^{15}N$ REDOR experiment and by a 2D relayed anisotropy correlation of the $^{13}C'$ CSA ($\omega_2$) and $^{15}N$-$^{1}H$ dipolar interaction ($\omega_1$). Via numerical simulations the sensitivity of the $\omega_1$ cross sections of the 2D spectrum to the Euler angles of the $^{15}N$-$^{1}H$ bond vector in the $^{13}C'$ CSA frame is shown. Employing the procedure outlined in this work, we have determined the orientation of the $^{13}C'$ CS tensor in the peptide plane of the dipeptide AibAib-$NH_2$ (Aib = α-aminoisobutyric acid). The Euler angles are found to be ($\chi_{CN}$, $\psi_{CN}$) = (34° ± 2°, 88° ± 2°) and ($\chi_{NH}$, $\psi_{NH}$) = (90° ± 10°, 80° ± 10°). From the measured Euler angles it is seen that the $\sigma_{33}$ and $\sigma_{22}$ components of the $^{13}C'$ CS tensor approximately lie in the peptide plane.

## Introduction

In the study of membrane-bound peptides and proteins, solid state NMR is emerging as a powerful source of structural information (Opella, 1997; Smith et al., 1996; Marassi and Opella, 1998; Fu and Cross, 1999). It is seen that a knowledge of the magnitude and orientation of chemical shift (CS) tensors, for example of the $^{15}N$ and $^{13}C'$ nuclei in the peptide backbone, is often essential in these investigations. Structural studies of membrane-bound peptides and proteins can be carried out via two different high resolution solid state NMR approaches. One approach relies on orienting the sample of peptides/proteins embedded in lipid bilayers mechanically (Opella et al., 1987) or magnetically (Sanders et al., 1994) with respect to the external magnetic field. In such experiments, the observed spectral parameters such as chemical shift and dipolar couplings are dependent upon the orientation of the relevant nuclear spin interaction tensor relative to the magnetic field. From a knowledge of the magnitude and orientation of the relevant CS tensor in the peptide plane, the observed chemical shift in a spectrum of an oriented sample can be analyzed in terms of the orientation of the peptide planes with respect to the magnetic field. Information about the secondary structure of the peptide backbone can then be obtained from the respective orientations of all peptide planes relative to the magnetic field (Ketchem et al., 1993; North et al., 1995; Kovacs and Cross, 1997; Bechinger et al., 1998).

Alternatively, obtaining structural data from solid state NMR involves the study under magic angle spinning (MAS) of unoriented crystalline powders (Schmidt-Rohr and Spiess, 1994; Griffin, 1998; Shaw et al., 2000) and powder-like specimens, e.g. pep-

*To whom correspondence should be addressed. E-mail: raman@imb-jena.de

tides in a multilamellar lipid dispersion (Hing and Schaefer, 1993; Hirsh et al., 1996) and frozen protein solution (Li et al., 1995). Homo- and heteronuclear dipolar recoupling techniques (Bennett et al., 1994; Griffin, 1998) are employed to inhibit the spatial averaging of weak dipolar couplings under MAS and structural constraints are obtained as distances and torsion angles. The data analysis of some of these techniques requires a knowledge of the orientation of the $^{15}$N and $^{13}$C′ chemical shift tensors, e.g. in the peptide plane. For example, Bower et al. (1999) have recently shown a method for obtaining the Ramachandran angles ($\phi$,$\psi$) via DRAWS (Gregory et al., 1995) and DQDRAWS (Gregory et al., 1997) experiments on carbonyl $^{13}$C-labelled peptides. This method requires a knowledge of the $^{13}$C′ CS tensor orientation in the peptide plane (Bower et al., 1999) and an accurate measurement of torsion angles would be facilitated if exact CS tensor orientational parameters were available.

Information about the CS tensor orientation in the molecular frame can also be useful in other investigations such as solution state NMR studies involving cross correlated relaxation processes (Yang et al., 1997; Yang and Kay, 1998; Pang et al., 1999; Pellechia et al., 1999; Reif et al., 2000).

Solid state NMR has been the traditional method of choice for the characterization of CS tensor parameters. For such investigations, techniques which are based on polycrystalline materials and techniques which are convenient to implement (Linder et al., 1980; Hartzell et al., 1987a,b; Oas et al., 1987; Teng and Cross, 1989; Teng et al., 1992) and techniques based on single crystals (Harbison et al., 1984; Takeda et al., 1999) have been proposed. Compared to static methods, MAS NMR studies provide better sensitivity and resolution and hence, MAS NMR is the method of choice in the study of powder specimens. While the magnitude of the CS tensor principal values can be conveniently obtained from conventional CPMAS studies on polycrystalline samples (de Groot et al., 1991; Schmidt-Rohr and Spiess, 1994), extraction of CS tensor orientations is not straightforward. To orient a CS tensor in the local molecular frame, for example a peptide plane, one can measure the Euler angles of two dipolar vectors in the CS tensor principal axes system (Hartzell et al., 1987a). For example, for backbone $^{15}$N nuclei we have shown that one can effectively use $^{15}$N-$^{13}$C REDOR (Gullion and Schaefer, 1989; Goetz and Schaefer, 1997) and $^{15}$N-$^{1}$H DIPSHIFT (Munowitz and Griffin, 1982, 1983) experiments to obtain the necessary Euler angles (Heise et al., 2000; Leppert et al., 2000a). When dealing with a dipolar network of the type $^{15}$N1-$^{13}$C-$^{15}$N2, as, e.g., in the bases of nucleic acids, we have shown that a $^{13}$C-$^{15}$N REDOR (Leppert et al., 2000b) or a $^{15}$N $\rightarrow$ $^{13}$C TEDOR experiment (Leppert et al., 2001) can be effectively employed to determine the $^{13}$C′ CS tensor orientation in the molecular frame spanned by the two dipolar vectors C-N1 and C-N2.

In this work, we suggest a method for obtaining the CS tensor orientation of the carbonyl $^{13}$C CS tensor in a $^{13}$C′-$^{15}$N-$^{1}$H dipolar network, for example of a carbonyl carbon in the backbone of peptides and proteins or of the carbons in nucleic acid bases, e.g., uridine (C4) and guanine (C6). The method involves the determination of the Euler angles ($\chi_{CN}$, $\psi_{CN}$) of the $^{13}$C′-$^{15}$N dipolar vector in the $^{13}$C′ CS tensor frame from a $^{13}$C-$^{15}$N REDOR experiment and the angles ($\chi_{NH}$, $\psi_{NH}$) of the $^{15}$N-$^{1}$H vector via a relayed anisotropic correlation of the $^{13}$C′ CSA with the $^{15}$N-$^{1}$H dipolar interaction. In the context of the determination of the peptide torsion angle $\varphi$, Hong et al. (1998) have recently proposed, considering a $^{1}$H-$^{15}$N-$^{13}$C$_\alpha$-$^{1}$H spin network, a 2D approach for correlating the $^{15}$N CS and $^{13}$C$_\alpha$-$^{1}$H dipolar tensor interactions. In this approach, the orientational information is obtained from a single $\omega_1$ cross section. This cross section, containing information about the sum and difference frequencies of the relevant chemical shift and dipolar couplings, is taken at the isotropic $^{13}$C$_\alpha$ position in $\omega_2$. In principle, the method of Hong et al. (1998) could be adapted to correlate the $^{13}$C′ chemical shift and $^{15}$N-$^{1}$H dipolar interactions in the peptide backbone. However, in this work we have taken the alternative approach of extracting the relative orientation of tensorial interactions via a 2D correlation of the relevant anisotropic interactions (Linder et al., 1980; Munowitz and Griffin, 1982, 1983). This method makes use of the fact that each of the $\omega_1$ cross sections running through the centreband or sidebands of the $^{13}$C′ chemical shift spectrum in the $\omega_2$ dimension reflects the orientational relationship between the dipolar and chemical shift interactions. A $^{15}$N $\rightarrow$ $^{13}$C TEDOR coherence transfer step (Hing et al., 1992, 1993) is employed to obtain a 2D correlation of the $^{15}$N-$^{1}$H dipolar ($\omega_1$) and $^{13}$C′ chemical shift ($\omega_2$) tensor interactions. The potential of 2D relayed anisotropic correlation experiments for obtaining orientational information has been pointed out earlier in the literature (Ishii et al., 1996; Takegoshi et al., 2000). However, the approach adopted here does not result in 2D powder patterns under MAS but in-

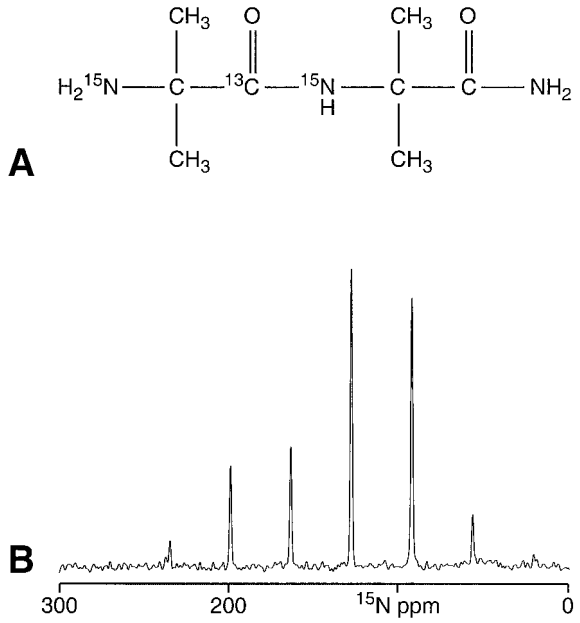


*Figure 1.* (A) AibAib dipeptide with ($^{15}$N, $^{13}$C′) labelling at positions indicated. (B) Typical $^{15}$N CPMAS spectrum of AibAib ($\nu_r$ = 1800 Hz).

stead leads to 2D data with spectral peaks occurring only at integral multiples of the spinning speed and thereby facilitates rapid spectral data analysis. In our scheme, the $^{15}$N → $^{13}$C TEDOR polarization transfer step is preceded by a $^{15}$N-$^{1}$H dipolar evolution time. The sensitivity of the dipolar sideband patterns to the Euler angles ($\chi_{NH}$, $\psi_{NH}$) is shown via numerical simulations. From a determination of the Euler angles ($\chi_{CN}$, $\psi_{CN}$) and ($\chi_{NH}$, $\psi_{NH}$), we have obtained the $^{13}$C′ CS tensor orientation in the peptide plane of an AibAib dipeptide (Figure 1A), where Aib represents the unusual amino acid α-aminoisobutyric acid which is present in many channel forming peptaibols such as alamethicin and the chrysospermins.

Peptaibols are ion channel forming polypeptides containing a high percentage of Aibs as one of the constituents (Benedetti et al., 1982; Sansom, 1993a,b). Due to e.g. their antibacterial and fungicidal activities, structural studies of peptaibols are of considerable current research interest. The 19-residue peptaibol chrysospermin C, isolated from the fungus *Apiocrea chrysosperma* (Dornberger et al., 1995), is one of the systems which is currently being studied via NMR in our laboratory (Anders et al., 1998, 2000). Chrysospermin C is an example of an ion channel in which channel activity is observed for salt concentration gradients even without electrical potential applied across the bilayer (Grigoriev et al., 1995; Ternovsky et al., 1997). Solution state NMR studies of chrysospermin C in a micellar environment indicate that chrysospermin C consists of an N- and C-terminal helix separated by a slight central bend (Anders et al., 2000). We are currently pursuing solid state NMR studies on chrysospermin C bound to magnetically oriented DHPC/DMPC bicelles to obtain the orientation of the peptide with respect to the bilayer surface. For the interpretation of the observed chemical shift in such experiments, as mentioned earlier, a knowledge of the relevant CS tensor magnitudes and orientations is crucial. $^{15}$N and $^{13}$C′ CS tensor parameters are currently available for a variety of amino acid dipeptides (Oas et al., 1987; Shoji et al., 1993), but no data is available on systems containing the unusual amino acid Aib. To obtain data on $^{13}$C′ CS tensor parameters in Aib-containing systems we have carried out measurements on a $^{15}$N, $^{13}$C′ labelled AibAib dipeptide (Figure 1A).

## Experimental

*Synthesis of labelled AibAib dipeptide*

$^{15}$N-labelled Fmoc-Aib-OH (5 equiv, related to the maximum resin capacity) was preactivated with *N*-[(dimethylamino)-1H-1,2,3-triazolo-[4,5-*b*]pyridin-1-ylmethylene]-*N*-methylmethanaminium hexafluorophosphate *N*-oxide (HATU) (5 equiv) and diisopropylethylamine (DIEA) (10 equiv) in dimethylformamide (DMF; concentration: 0.5 M) for 10 min and coupled to 1 g of a Rink amide NovaGel HL resin (loading: 0.6 mmol/g; Novabiochem, Bad Soden, Germany). The reaction was performed via double coupling (1 h each). The resin was washed with DMF (3 × 1 min, 10 ml each) and the Fmoc group was deblocked by treatment with 10 ml 20% piperidine/DMF for 20 min. After washing with DMF (5 × 1 min, 10 ml each) Fmoc-Aib-OH, $^{13}$C, $^{15}$N-labelled at the carboxy function, was coupled in the same manner. The resin was then washed with DMF (3 × 1 min, 10 ml each) and the Fmoc group was deblocked as before. Washing with DMF (5 × 1 min, 10 ml each), and dichloromethane (DCM; 3 × 1 min, 10 ml each) was followed by peptide resin cleavage with 50% trifluoroacetic acid (TFA)/DCM containing 5% water for 2 h. After evaporation of TFA and DCM the peptide was lyophylized and purified by preparative HPLC using a Vydac C18 column. ESI-MS: calculated: 188.15 (monoisotopic); found: 189.5 $[M^+H]^+$.

*Solid state NMR spectroscopy*

All experiments were performed at room temperature on a wide bore Varian $^{\mathrm{UNITY}}$INOVA 500 MHz solid state NMR spectrometer equipped with 5 mm supersonic DOTY triple resonance probes. Cross-polarization under Hartmann–Hahn matching conditions was used to enhance the sensitivity of all spectra employing typical $^{1}$H, $^{13}$C and $^{15}$N 90° pulse widths of 3.8, 4.5 and 7.3 μs, respectively. Standard pulse sequences were employed for obtaining the $^{13}$C CPMAS and $^{13}$C-$^{15}$N REDOR spectra of the dipeptide. $^{15}$N CPMAS spectra only show the signal from the amide nitrogen (Figure 1B). The N-terminal $^{15}$N ($NH_2$) signal could be observed only as a broad hump (reasons unknown) around 50 ppm in CPMAS spectra acquired at very low spinning speeds below 1 kHz (data not shown). In the 2D correlation of the $^{13}$C′ CSA with $^{15}$N-$^{1}$H dipolar interaction via the pulse sequence given in Figure 2, standard phase cycling procedures were employed to eliminate the contribution from signals arising from unwanted coherence transfer pathways. The $^{15}$N transverse magnetization present at the end of the cross polarization period is allowed to evolve in $t_1$ under the scaled $^{15}$N-$^{1}$H dipolar coupling and is then subsequently transferred to the $^{13}$C′ spins via a TEDOR coherence transfer step. As one is dealing with directly connected $^{15}$N and $^{13}$C′ spins, only two rotor periods of dipolar recoupling before and after the polarization transfer step were used to achieve efficient coherence transfer at the spinning speeds employed in this work. A 90° pulse in the $^{15}$N channel and at the start of the $^{13}$C data acquisition is employed to purge the contributions from anti-phase operator terms to the observed signal (Heise et al., 2000; Leppert et al., 2000b). Unless mentioned otherwise, all spectra were collected under high power TPPM $^{1}$H decoupling (Bennett et al., 1995). Homonuclear $^{1}$H decoupling, where required, was achieved by employing a semi-windowless MREV8 sequence (Rhim et al., 1973). 2D data sets with normal and time reversed dipolar evolution (Munowitz and Griffin, 1983) were collected to generate phase sensitive relayed anisotropy correlation NMR spectra. All spectra were referenced indirectly to DSS (Wishart et al., 1995).

## Calculations

Extraction of CS tensor principal values from CPMAS data and orientational information from REDOR spectra was carried out as described earlier employing the software package 'SPINME' (Leppert et al., unpublished; Heise et al., 2000; Leppert et al., 2000b). Considering the spin 1/2 dipolar network $^{1}$H-$^{15}$N-$^{13}$C′, we have carried out density matrix calculations to compute 2D relayed anisotropic correlation spectra. In these calculations we have neglected scalar couplings and assumed ideal experimental conditions. For a single crystallite, specified by the Euler angles (α, β, γ) defining the orientation of the $^{13}$C′ CS tensor principal axes system in the rotor frame, the observed signal (forward dipolar evolution) at a MAS frequency $\omega_r$ is given by:

$$\left\langle I^{+}\left(t_1, t_2\right)\right\rangle = \sin^2 A \cdot \cos E_f \cdot \cos B \cdot \exp\left(iC\right),$$

where

$$A = 4D_{CN}\left(\frac{\omega_{CN}}{\omega_r}\right)\sin\alpha_{D_{CN}}$$

$$\begin{aligned} E_f = \frac{\omega_{NH}}{4\omega_r}\big[&2D_{NH}\sin\left(\omega_r t_1 - \alpha_{D_{NH}}\right) \\ &+ G_{NH}\sin 2\left(\omega_r t_1 - \alpha_{D_{NH}}\right) \\ &+ 2D_{NH}\sin\alpha_{D_{NH}} \\ &+ G_{NH}\sin 2\alpha_{D_{NH}}\big] \end{aligned}$$

$$\begin{aligned} B = \frac{\omega_{CN}}{4\omega_r}\big[&2D_{CN}\sin\left(\omega_r t_2 - \alpha_{D_{CN}}\right) \\ &+ G_{CN}\sin 2\left(\omega_r t_2 - \alpha_{D_{CN}}\right) \\ &+ 2D_{CN}\sin\alpha_{D_{CN}} \\ &+ G_{CN}\sin 2\alpha_{D_{CN}}\big] \end{aligned}$$

and

$$\begin{aligned} C = \frac{\omega_I}{2\omega_r}\big[&(2g_1\sin\phi_1 + g_2\sin\phi_2) \\ &- (2g_1\sin\left(\omega_r t_2 + \phi_1\right) \\ &+ g_2\sin\left(2\omega_r t_2 + \phi_2\right))\big] \end{aligned}$$

In the above equations, we have $D_{CN} = 2\sqrt{2}\sin\beta_{D_{CN}}\cos\beta_{D_{CN}}$, $G_{CN} = \sin^2\beta_{D_{CN}}$ and $\omega_I = \omega_0[\sigma_{33} - 1/3(\sigma_{11} + \sigma_{22} + \sigma_{33})]$ with $\sigma_{ii}$ $(i = 1, 2, 3)$ representing the $^{13}$C′ CS tensor principal values. $D_{NH}$ and $G_{NH}$ are defined similar to $D_{CN}$ and $G_{CN}$. $\omega_{CN}$ and $\omega_{NH}$ are the dipolar coupling strengths, $(\beta_{D_{CN}}, \alpha_{D_{CN}})$ and $(\beta_{D_{NH}}, \alpha_{D_{NH}})$ are the Euler angles of the $^{13}$C′-$^{15}$N and $^{15}$N-$^{1}$H dipolar vectors in the rotor frame and $g_1$, $g_2$, $\phi_1$ and $\phi_2$ are as defined before (Leppert et al., 1999). The Euler angles of the dipolar vectors in the rotor frame are related to the Euler angles $(\chi_{CN}, \psi_{CN})$ and $(\chi_{NH}, \psi_{NH})$ in the $^{13}$C′ CS tensor principal axes system via (α, β, γ). In our notation, $\sigma_{33}$ denotes the

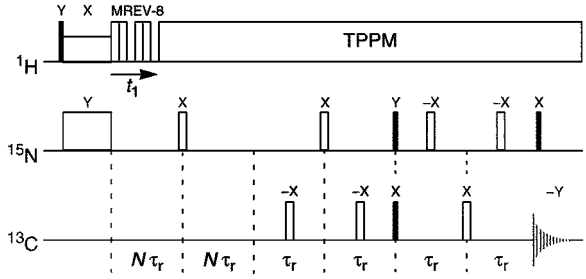


*Figure 2.* Pulse sequence employed for 2D correlation of the $^{15}$N-$^{1}$H dipolar (forward evolution) and $^{13}$C′ CSA interactions. All 180° pulses were applied either at the centre or the end of the rotor periods, as shown.

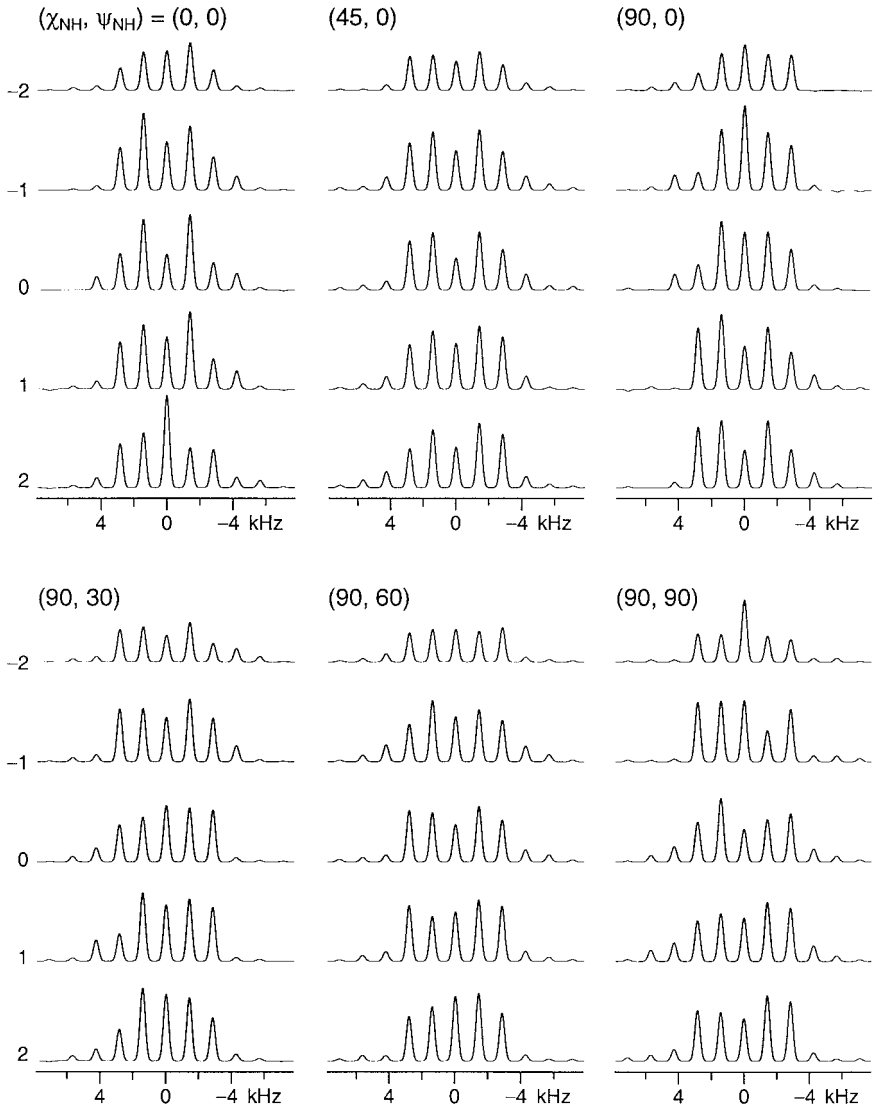


*Figure 3.* Simulated $\omega_1$ dipolar cross sections (at the $\omega_2$ side-band positions indicated) of the 2D relayed anisotropic correlation spectra at a spinning speed of 1400 Hz and as a function of a coarse variation of the Euler angles ($\chi_{NH}$, $\psi_{NH}$), as indicated. These plots were generated employing $^{13}$C′ CS tensor principal values of $(\sigma_{11}, \sigma_{22}, \sigma_{33}) = (92.1 \text{ ppm}, 191.4 \text{ ppm}, 239.1 \text{ ppm})$, a $^{15}$N-$^{13}$C′ dipolar coupling strength of 1200 Hz, a scaled $^{15}$N-$^{1}$H dipolar coupling strength of 5500 Hz and Euler angles ($\chi_{CN}$, $\psi_{CN}$) of (34°, 88°).

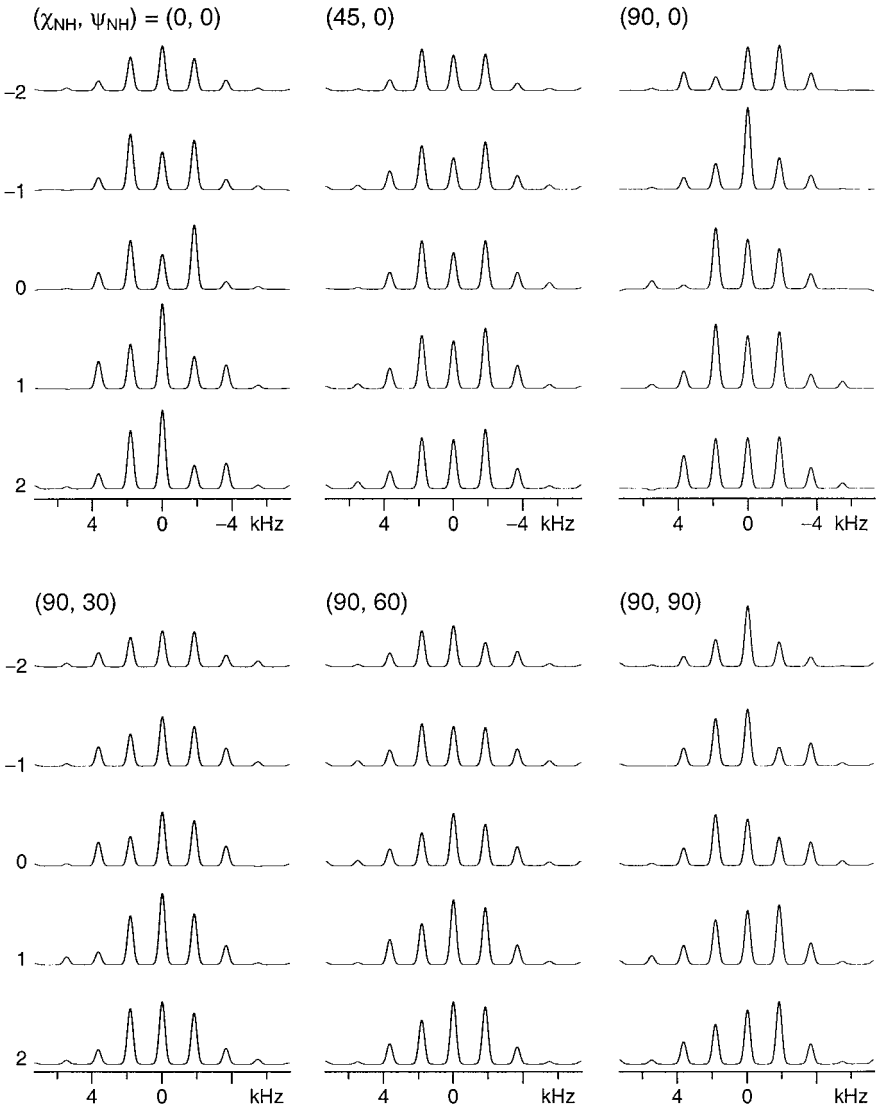


*Figure 4.* Simulated $\omega_1$ dipolar cross sections (at the $\omega_2$ side-band positions indicated) of the 2D relayed anisotropic correlation spectra at a spinning speed of 1800 Hz and as a function of a coarse variation in the Euler angles ($\chi_{NH}$, $\psi_{NH}$) indicated. All other parameters employed in the simulations were the same as given in Figure 3.

least shielded component of the CS tensor, $\chi$ represents a rotation about $\sigma_{22}$ and $\psi$ defines a subsequent rotation about $\sigma_{33}$. Parameters such as the $^{13}C'$-$^{15}N$ dipolar coupling strengths and the Euler angles of the $^{13}C'$-$^{15}N$ dipolar vector in the $^{13}C'$ CSA frame which are needed in the calculation of the 2D spectral data can be obtained from other measurements and these are employed in our calculations. A weighted averaging of the response over all possible crystallite orientations gives the final signal observed.

**Results**

The sensitivity of the dipolar sideband patterns of the 2D relayed anisotropic correlation NMR spectra to the Euler angles ($\chi_{NH}$, $\psi_{NH}$) has been assessed by simulating the spectrum as a function of the angles at different spinning speeds. In Figures 3 and 4 we show the $\omega_1$ cross sections for coarse variations in the Euler angles at two representative spinning speeds of 1400 and 1800 Hz, respectively. The effect of finer variations in the angles on the observed side-band intensity patterns is shown in Figure 5 for a spinning

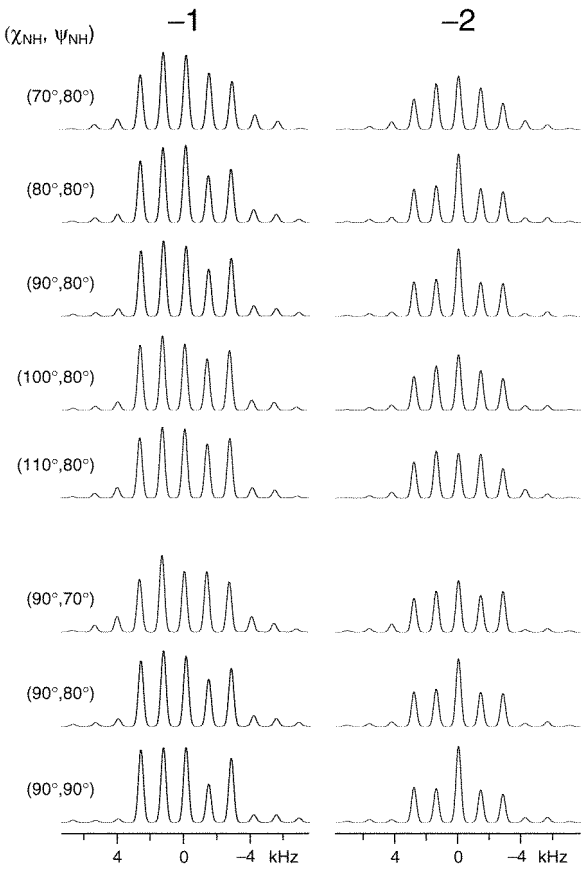


*Figure 5.* Simulated $\omega_1$ dipolar cross sections (at the $\omega_2$ side-band positions indicated) of the 2D relayed anisotropic correlation spectra at a spinning speed of 1400 Hz with finer variations in the Euler angles ($\chi_{NH}$, $\psi_{NH}$). The angles are varied around the values observed experimentally in the dipeptide. All other parameters employed in the simulations were the same as given in Figure 3.

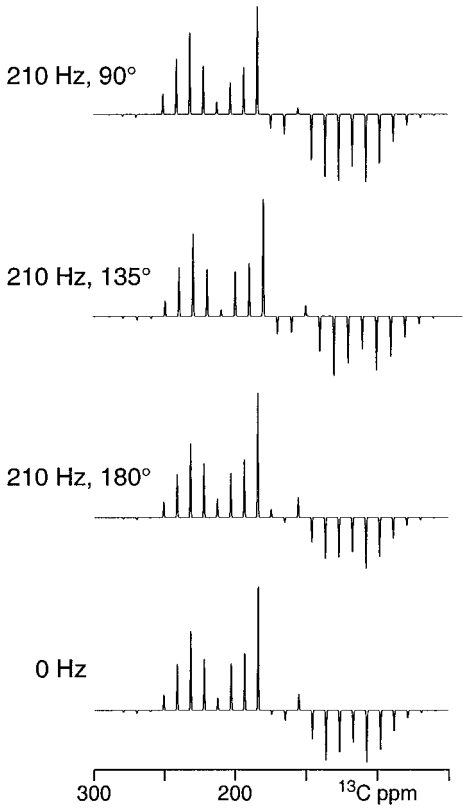


*Figure 6.* Simulated two-rotor period, purged $^{13}$C-$^{15}$N REDOR spectra at a spinning speed of 1200 Hz displaying the influence of the second amide nitrogen at two-bond distance. These plots were generated for different polar angles $\chi_{CN2}$ using a two-bond dipolar coupling of 210 Hz and ($\chi_{CN}$, $\psi_{CN}$) of (34°, 88°). A spectrum generated neglecting the two-bond coupling is also shown (bottom).

speed of 1400 Hz. These spectra were generated employing the $^{13}C'$ CS tensor principal values, $^{13}C'$-$^{15}$N and $^{15}$N-$^{1}$H dipolar coupling strengths and Euler angles ($\chi_{CN}$, $\psi_{CN}$) as found for the AibAib dipeptide (see below). From these plots it is seen that the dipolar sideband patterns are sensitive to the Euler angles ($\chi_{NH}$, $\psi_{NH}$). For smaller variations in ($\chi_{NH}$, $\psi_{NH}$), even if the differences in the dipolar sideband intensity patterns are not very pronounced in one of the $\omega_1$ cross sections, measurable variations can still be seen in some other cross section of the 2D spectrum. From the results presented it can be concluded that the pulse sequence given in Figure 2 can be conveniently employed to extract the Euler angles ($\chi_{NH}$, $\psi_{NH}$). For obtaining the $^{13}C'$ CS tensor orientation, both Euler angle pairs ($\chi_{CN}$, $\psi_{CN}$) and ($\chi_{NH}$, $\psi_{NH}$) are required. From our simulations (data not shown) it could be deduced that the two-dimensional cross sections were not sensitive to ($\chi_{CN}$, $\psi_{CN}$) and hence, these angles have to be determined via some other experiment. We have obtained these angles via $^{13}$C- $^{15}$N REDOR.

Since in our AibAib dipeptide two nitrogen sites are isotopically labelled (Figure 1A), we have assessed the possible influence of the two-bond coupled nitrogen on the observed REDOR sideband intensities. Figure 6 shows simulated purged two-rotor period $^{13}$C-$^{15}$N REDOR spectra of a three-spin $^{15}$N1-$^{13}$C $\cdots$ $^{15}$N2 dipolar network. These plots were generated employing one- and two-bond $^{13}C'$-$^{15}$N dipolar coupling strengths of 1200 and 210 Hz, respectively (distances 1.36 Å, 2.43 Å). It was seen from spectral simulations that the side-band intensity patterns for the one- ($1\tau_r$) and two-rotor period ($2\tau_r$) REDOR experiments carried out in this work are not affected by variations in the two-bond dipolar coupling strength in the expected range of 190–230 Hz (simulations not shown).

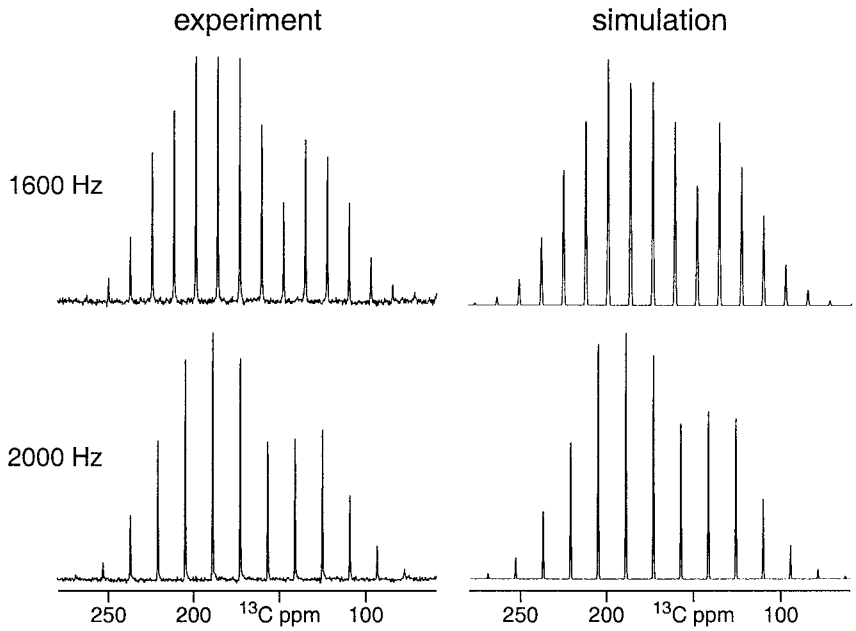


*Figure 7.* Experimental and simulated $^{13}$C CPMAS data of the ($^{15}$N,$^{13}$C′) labelled dipeptide at spinning speeds of 1600 and 2000 Hz. The experimental spectra were recorded using a conventional CPMAS sequence. The simulated spectra were generated employing the optimized CS tensor parameters of $(\sigma_{11}, \sigma_{22}, \sigma_{33}) = (92.1 \text{ ppm}, 191.4 \text{ ppm}, 239.1 \text{ ppm})$, a $^{13}$C′-$^{15}$N dipolar coupling strength of 1200 Hz and Euler angles ($\chi_{CN}$, $\psi_{CN}$) of (34°, 88°).

Hence, a value of 210 Hz was employed for the two-bond dipolar coupling. Since the REDOR side-band intensities were not found to be sensitive to the azimuthal angle $\psi_{CN2}$ of the two-bond dipolar vector in the $^{13}$C′ CS tensor frame, these plots were generated for some representative values of the polar angle $\chi_{CN2}$. For comparison, a spectrum generated neglecting the two-bond dipolar coupling is also shown in Figure 6. These plots show that the presence of the two-bond dipolar coupling can lead to some variations in the observed side-band intensity patterns. Hence, the iterative analysis of the experimental REDOR spectra (see below) and the REDOR spectral simulations were carried out by considering a three-spin dipolar network (Leppert et al., 2000b).

Extraction of orientational information from $^{13}$C-$^{15}$N REDOR and 2D relayed anisotropic spectra requires the values of the CS tensor principal elements and $^{15}$N-$^{13}$C′ dipolar coupling strength. The analysis of the 2D data additionally requires the values of ($\chi_{CN}$, $\psi_{CN}$). To obtain the CS tensor principal values, experimental $^{13}$C CPMAS spectra of the $^{15}$N, $^{13}$C′-labelled dipeptide were recorded at different spinning speeds at room temperature and the spectra at two representative spinning speeds are given in Figure 7. The $^{13}$C′-$^{15}$N dipolar coupling has been measured to be 1.2 kHz via $^{15}$N-$^{13}$C REDOR (data not shown). To obtain the angles ($\chi_{CN}$, $\psi_{CN}$), $^{13}$C-$^{15}$N purged REDOR spectra (Heise et al., 2000) were collected at different spinning speeds and with one and two rotor periods of dipolar recoupling; Figure 8 shows some typical spectra. The CPMAS and REDOR data were iteratively analyzed to obtain the optimal $^{13}$C′ CS tensor principal values and Euler angles ($\chi_{CN}$, $\psi_{CN}$) which lead to a satisfactory fit of both spectral data sets. In the estimation of the CS tensor principal values the effect of the one- bond $^{15}$N-$^{13}$C′ heteronuclear dipolar interaction, although found to be minimal, was also taken into consideration. The $^{13}$C′ CS tensor principal values were found to be $(\sigma_{11}, \sigma_{22}, \sigma_{33}) = (92.1 \text{ ppm}, 191.4 \text{ ppm}, 239.1 \text{ ppm})$ and the Euler angles ($\chi_{CN}$, $\psi_{CN}$) were determined as $(34° \pm 2°, 88° \pm 3°)$. A three-spin analysis of the REDOR data resulted in a value of $\chi_{CN2} = (143° \pm 12°)$. An analysis of the REDOR data shown in Figure 8 without considering the two-bond dipolar interaction also essentially leads to the same values for ($\chi_{CN}$, $\psi_{CN}$). The accuracy of the estimated parameters can be seen from the satisfactory fit of the experimental and simulated plots shown in Figures 7 and 8.

To obtain ($\chi_{NH}$, $\psi_{NH}$), 2D relayed spectra were collected at different spinning speeds and Figure 9

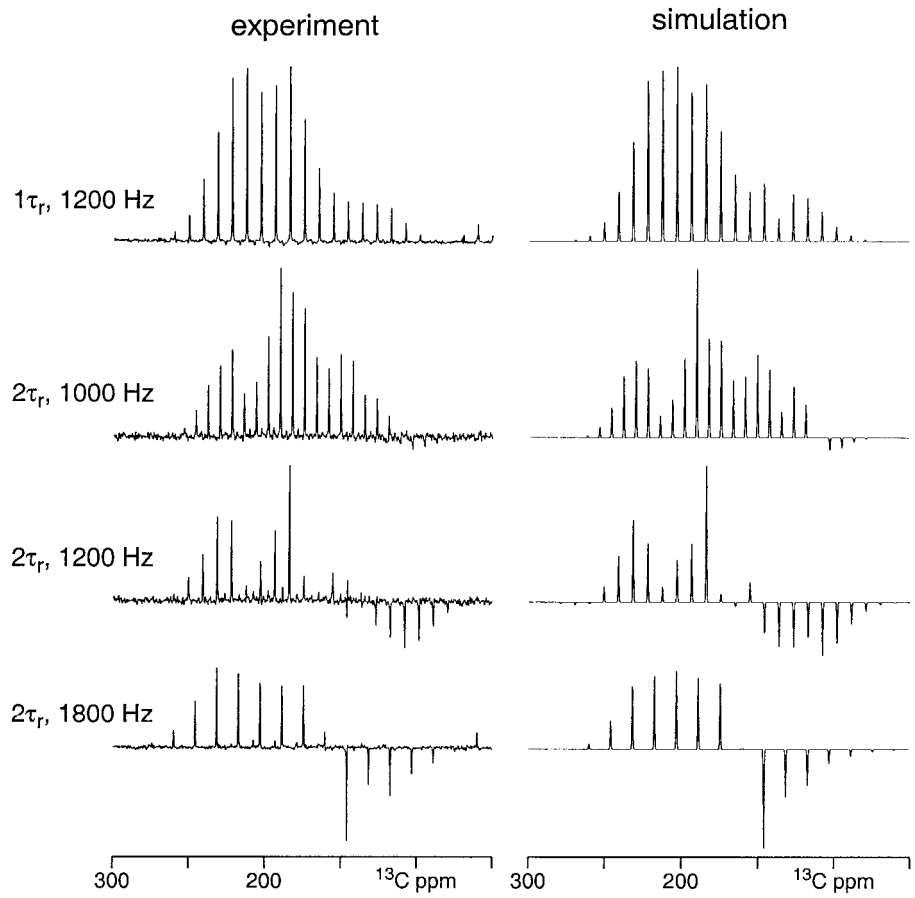


*Figure 8.* Experimental and simulated purged $^{13}C$-$^{15}N$ REDOR spectra of AibAib with one (Heise et al., 2000) and two rotor periods of dipolar recoupling (Leppert et al., 2000a) at various spinning speeds. Experimental spectra were recorded with the application of a 90° purging pulse in the $^{15}N$ channel at the start of the data acquisition (Heise et al., 2000; Leppert et al., 2000b), 8192 ($2\tau_r$, 1000 Hz, 1 and 2 $\tau_r$, 1200 Hz) and 4096 scans ($2\tau_r$, 1800 Hz) and a recycle time of 2 s. Simulated spectra were generated considering a three-spin dipolar network (Leppert et al., 2000b) employing the best fitting Euler angles ($\chi_{CN}$, $\psi_{CN}$) and $^{13}C'$ CS tensor principal values given in Table 1 and one- and two-bond $^{13}C'$-$^{15}N$ dipolar coupling strengths of 1200 Hz and 210 Hz, respectively.

shows the data for two representative spinning speeds. The dipolar cross sections were analyzed by computing the 2D spectra for various values of the Euler angles ($\chi_{NH}$, $\psi_{NH}$). The observed signal in the 2D experiment could originate, in principle, from both $^{15}N$ labelled sites. The $^{15}N$ signal from the N-terminal $NH_2$ site appears only in very low spinning speed CP-MAS data as a broad component and this site also experiences only a weaker two-bond heteronuclear dipolar coupling with the $^{13}C'$ spin. Hence, the contribution from this site is expected to be minimal and the observed signal should primarily arise from the one-bond coupled amide $^{15}N$ nitrogen. In the analysis of the signal arising from the directly coupled amide $^{15}N \rightarrow {}^{13}C'$ TEDOR transfer, one should also consider, in principle, the two-bond dipolar coupling interaction. However, as in the REDOR case, the effect of the two-bond heteronuclear dipolar coupling on the estimated Euler angles is not expected to be significant. Hence, to simplify our calculations, the experimental 2D cross sections were analyzed neglecting the two-bond $^{15}N$-$^{13}C'$ dipolar interaction. The spectral simulations were first carried out by incrementing the angles in coarse steps of ±30° to get an idea about the possible region in parameter space in which one may find the correct values for the Euler angles. The Euler angles are then varied in finer increments (± 5°) to get the best fitting values of the angles. Visual inspection reveals a satisfactory fit between the experimental and simulated data with ($\chi_{NH}$, $\psi_{NH}$) values of (90° ± 10°, 80° ± 10°). Figure 9 also shows the simulated cross sections obtained employing these values. All measured values

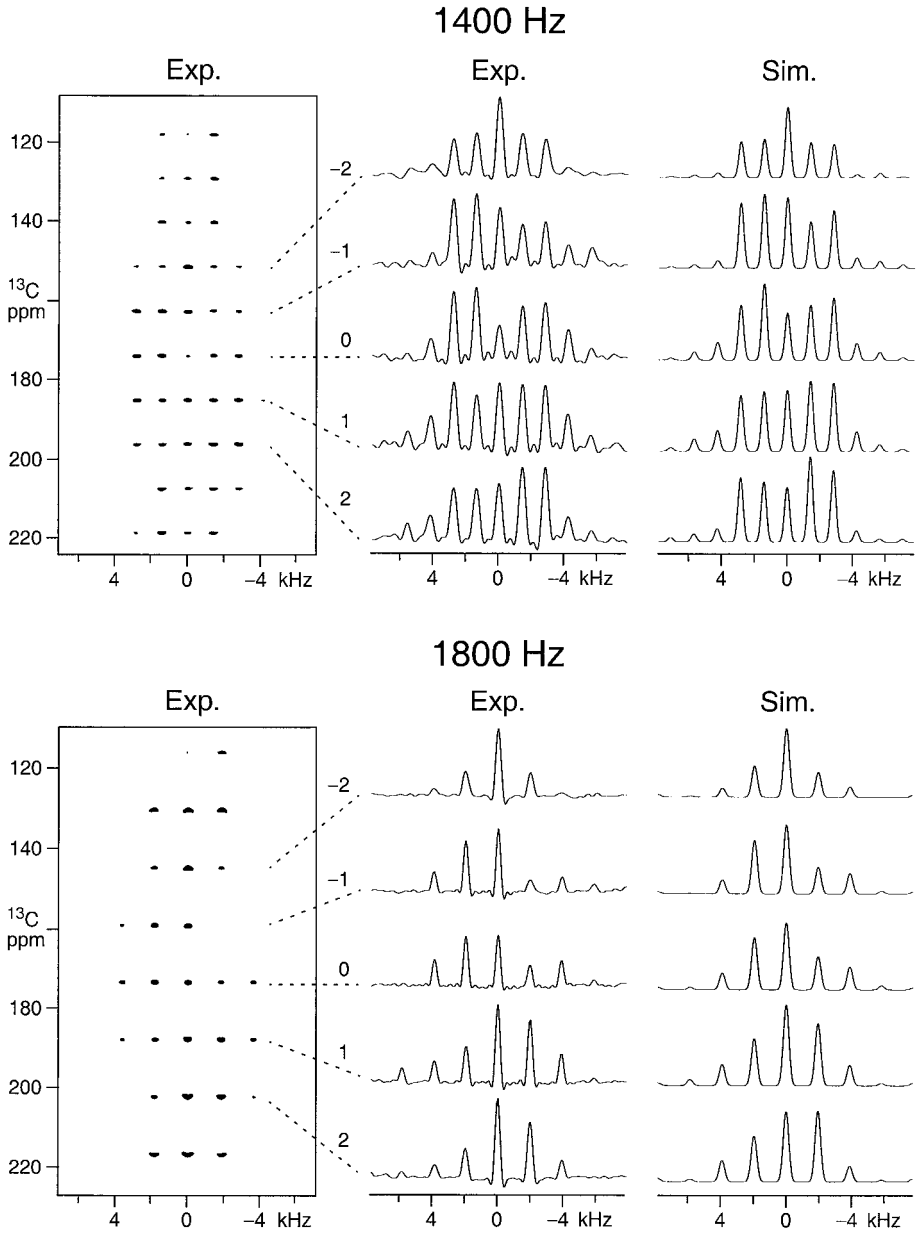


*Figure 9.* Experimental 2D relayed anisotropic correlation spectra of the dipeptide and the corresponding experimental and simulated dipolar cross sections. The experimental spectra at spinning speeds of 1400 Hz and 1800 Hz were generated employing the pulse sequence given in Figure 2 with N = 6 (1400 Hz) and 10 (1800 Hz). The simulated cross sections were obtained employing the estimated $^{13}C'$ CS tensor principal values, $^{13}C'$-$^{15}N$ dipolar coupling strength, mean Euler angles ($\chi_{CN}$, $\psi_{CN}$) from Table 1 and with ($\chi_{NH}$, $\psi_{NH}$) = (90°, 80°). In generating the two experimental spectral data sets, different $^{1}H$ RF power levels were employed for MREV decoupling (due to unexpected hardware problems) and the spectra at 1400 and 1800 Hz could be satisfactorily simulated employing scaled $^{15}N$-$^{1}H$ dipolar coupling strengths of 5500 and 5000 Hz, respectively.

*Table 1.* $^{13}C'$ CS tensor parameters of Aib determined at different spinning speeds $\nu_r$

| | $^{13}C$ CPMAS | | | $^{15}N$-$^{1}H$ dipolar $\leftrightarrow$ $^{13}C'$ CSA correlation | | $1\tau_r$ / $2\tau_r$ $^{13}C$-$^{15}N$ REDOR[a] | | |
|---|---|---|---|---|---|---|---|---|
| $\nu_r$ (Hz) | $\sigma_{11}$ (ppm) | $\sigma_{22}$ (ppm) | $\sigma_{33}$ (ppm) | $\chi_{NH}$ (°)[b,c] | $\psi_{NH}$ (°)[b,c] | $\chi_{CN}$ (°)[c] | $\psi_{CN}$ (°)[c] | $\chi_{CN2}$ (°)[d] |
| 1000 | 95.5 | 188.4 | 238.7 | – | – | 31 / 38 | 90 / 90 | 155 / 146 |
| 1200 | 93.0 | 189.1 | 240.5 | 90 | 80 | 31 / 36 | 90 / 90 | 136 / 166 |
| 1400 | 92.3 | 191.2 | 239.1 | 90 | 80 | 33 / 35 | 90 / 81 | 129 / 153 |
| 1600 | 91.1 | 191.1 | 240.3 | 90 | 80 | 35 / 35 | 90 / 82 | 142 / 147 |
| 1800 | 90.6 | 191.8 | 240.2 | 90 | 80 | 33 / 36 | 90 / 88 | 143 / 138 |
| 2000 | 92.8 | 191.6 | 238.2 | 90 | 80 | 35 / 34 | 90 / 89 | – [e] / 122 |
| 2200 | 92.0 | 193.2 | 237.4 | – | – | – | – | – |
| 2400 | 91.6 | 194.9 | 236.1 | – | – | – | – | – |
| Mean | $92.1 \pm 1.5$[f] | $190.3 \pm 1.9$[f] | $239.8 \pm 1.5$[f] | $90 \pm 10$ | $80 \pm 10$ | $34 \pm 2$[g] | $88 \pm 3$[g] | $143 \pm 12$[g] |

[a] Data collected with one/two rotor periods of dipolar recoupling.
[b] Values and error margins obtained from visual fitting of all 2D cross sections at all spinning speeds.
[c] $(180 - \chi_{CN})$, $-\psi_{CN}$, $\pm(180 - \psi_{CN})$ and $(180 - \psi_{NH})$ are also allowed solutions.
[d] $\psi_{CN2}$ could not be determined due to poor angular sensitivity. A 210 Hz two-bond $^{15}N$-$^{13}C'$ dipolar coupling was employed in the three-spin REDOR calculation in addition to the 1200 Hz one-bond coupling.
[e] No stable solution was found from iterative fitting.
[f] Calculated from the mean anisotropy $\delta_a = \sigma_{33} - \sigma_{iso} = 64.9$ and asymmetry parameter $\eta = (\sigma_{22} - \sigma_{11})/(\sigma_{33} - \sigma_{iso}) = 1.53$, as the iterative fitting procedure did not include the isotropic chemical shift $\sigma_{iso} = 174.2$ ppm.
[g] Mean value taken over both $1\tau_r/2\tau_r$ REDOR experiments.

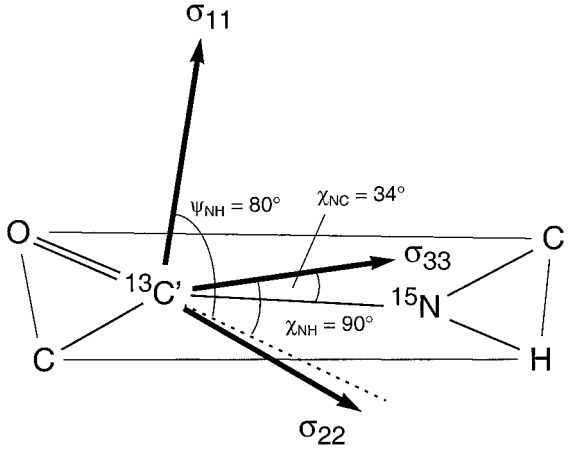


*Figure 10.* Orientation of the $^{13}C'$ CS tensor in the peptide plane of the AibAib dipeptide. The dashed line represents the direction of the N-H bond.

of the $^{13}C'$ CS tensor parameters in AibAib are given in Table 1. From the determined orientation of the N-H and N-C vectors in the $^{13}C'$ CS tensor principal axes system, one finds the orientation of the $^{13}C'$ CS tensor in the molecular frame of the peptide plane as depicted in Figure 10. As the angle included by the N-H and N-C′ bonds is ∼120° in a peptide, $\chi_{CN} = 34°$ and $\chi_{NH} = 90°$ place the least shielded CS tensor component $\sigma_{33}$ into the peptide plane. Experimental errors in the determination of $\chi_{CN}$ and $\chi_{NH}$, however, would allow $\sigma_{33}$ to move slightly out of the plane. The alignment of the most and intermediate shielded components $\sigma_{11}$ and $\sigma_{22}$ is given by the azimuthal angles $\psi_{CN}$ and $\psi_{NH}$. As $\sigma_{33}$ and the N-C′ and N-H bond vectors (the dotted line in Figure 10 is parallel to the N-H bond vector) are lying essentially in one plane, $\psi_{CN}$ and $\psi_{NH}$ should both have, in principle, the same value. This is confirmed, within the experimental error, by the estimated $\psi_{CN}$ and $\psi_{NH}$ values of ∼90° (Table 1). Since $\psi_{NH}$ is not exactly 90°, $\sigma_{11}$ is not perfectly perpendicular to the peptide plane and $\sigma_{22}$ is slightly tilted out of the peptide plane, deviating from the C′-O bond by ∼9°. The angle $\chi_{CN2} = 143° \pm 12°$, obtained from the three-spin analysis of the $^{13}C$-$^{15}N$ REDOR data, approximately fits with a torsion angle $\psi$ of −106°, as seen from molecular modelling.

## Discussion

From our studies it is seen that in a $^{13}C'$-$^{15}N$-$^{1}H$ dipolar network, the 2D relayed anisotropy correlation procedure can be effectively employed to obtain the orientation of the $^{15}N$-$^{1}H$ dipolar vector in the $^{13}C'$ CS tensor frame. This experiment, together with $^{13}C'$ CP-MAS and $^{13}C$-$^{15}N$ REDOR experiments, reveals that the magnitude and orientation of the CS tensor of the

carbonyl carbon in the peptide bond of the dipeptide AibAib do not deviate substantially from the typical values in commonly occurring amino acid dipeptides (Oas et al., 1987; Teng et al., 1992).

The pulse scheme employed in this work leads to 2D spectra displaying a matrix of rotational side-bands spaced at $\omega_r$ in both dimensions. Such 2D spectral data sets are amenable to a fast extraction of orientational parameters as the computation of such spectra only requires the calculation of the time domain data $S(t_1,t_2)$ over one rotor period. By making use of the periodicity of the Hamiltonian under MAS, the time domain data over one rotor period can be replicated to obtain, after Fourier transformation, 2D spectra with good spectral resolution (Hong et al., 1997a, 1998). In our case, the typical time required for the computation of one 2D data set on a SGI Origin R12000/270 computer is less than 10 s. Such fast computation permits the generation of a large number of spectra, corresponding to different values of the Euler angles, in a reasonable amount of time and thereby makes the analysis of the experimental spectra easier.

To achieve sufficient spectral resolution in the experimental $\omega_1$ cross sections, we have employed multiple rotor periods of dipolar evolution in the $t_1$ dimension of the 2D experiments. However, as in the numerical computation of 2D spectra, orientational information could also be extracted even from experimental data recorded during a single rotor period of dipolar evolution (Hong et al., 1997a, 1998). Like in the simulations, a replication of such reduced experimental data sets would have to be used to increase the spectral resolution. Such a restriction to one single rotor period of dipolar evolution could minimize signal loss due to $T_2$ relaxation and thereby improve the signal-to-noise ratio. The sensitivity of the dipolar cross sections of the relayed anisotropy data to the Euler angles ($\chi_{NH}$, $\psi_{NH}$) can possibly also be improved via an up-scaling of the $^{15}$N-$^{1}$H dipolar interaction (Hong et al., 1997b).

The procedure employed here can possibly also be employed for the characterization of the $^{13}$C′ CS tensor orientation in isotopically labelled nucleic acid bases, for example, of the C4 and C6 of the uridine and guanine RNA bases, respectively. These carbonyl carbons, through their directly attached oxygen, play an important role in hydrogen bonding. While we have shown earlier the possibilities to measure the 2-$^{13}$C CS tensor orientations of the pyrimidine bases via $^{13}$C-$^{15}$N REDOR or $^{15}$N $\rightarrow$ $^{13}$C TEDOR studies (Leppert et al., 2000b, 2001), the 2D relayed anisotropic correlation experiment outlined here can be employed for the characterization of the CS tensor orientation of the 4-$^{13}$C and 6-$^{13}$C of the uridine and guanine bases, respectively. The availability of efficient procedures for characterizing the CS tensor orientations of different sites in nucleic acid bases should permit a systematic study of hydrogen bonding effects on the CS tensors in nucleic acids (Czernek et al., 2000). This may allow to relate the measured CS tensor orientations and magnitudes to structural features. By incorporating suitable homonuclear $^{13}$C-$^{13}$C dipolar decoupling (Schaefer, 1999), the techniques employed here could also be extended to systems with multiple $^{15}$N and $^{13}$C labelled sites.

The approach of determining the Euler angles of two dipolar vectors to define the CS tensor orientation in the molecular frame (Hartzell et al., 1987a) was employed in this work. Alternatively, in situations where the CS tensor orientation of one of the nuclei in a heteronuclear dipolar coupled spin system is already available, the CS tensor orientation of the other nucleus can be obtained from a 2D relayed anisotropic correlation of the CSAs of the two nuclei. Such experiments are in progress in our laboratory.

## References


Anders, R., Ohlenschläger, O., Soskic, V., Wenschuh, H., Heise, B. and Brown, L.R. (2000) *Eur. J. Biochem.*, **267**, 1784–1794.

Anders, R., Wenschuh, H., Soskic, V., Fischer-Frühholz, S., Ohlenschläger, O., Dornberger, K. and Brown, L.R. (1998) *J. Pept. Res.*, **52**, 34–44.

Bechinger, B., Zasloff, M. and Opella, S.J. (1998) *Biophys. J.*, **74**, 981–987.

Benedetti, E., Bavoso, A., Di Blasio, B., Pavone, V., Pedone, C., Toniolo, C. and Bonora, G.M. (1982) *Proc. Natl. Acad. Sci. USA*, **79**, 7951–7954.

Bennett, A.E., Griffin, R.G. and Vega, S. (1994) *NMR Basic Principles and Progress*, Springer Verlag, Berlin, Vol. 33, pp. 1–77.

Bennett, A.E., Rienstra, C.M., Auger, M., Lakshmi, K.V. and Griffin, R.G. (1995) *J. Chem. Phys.*, **103**, 6951–6958.

Bower, P.V., Oyler, N., Mehta, M.A., Long, J.R., Stayton, P.S. and Drobny, G.P. (1999) *J. Am. Chem. Soc.*, **121**, 8373–8375.

Czernek, J., Fiala, R. and Sklenar, V. (2000) *J. Magn. Reson.*, **145**, 142–146.

Dornberger, K., Ihn, W., Ritzau, M., Gräfe, U., Schlegel, B., Fleck, W.F. and Metzger, J.W. (1995) *J. Antibiot.*, **48**, 977–989.

Fu, R. and Cross, T.A. (1999) *Annu. Rev. Biophys. Struct.*, **28**, 235–268.

Goetz, J.M and Schaefer, J. (1997) *J. Magn. Reson.*, **127**, 147–154.

Gregory, D.M., Mitchell, D.J., Stringer, J.A., Kiihne, S., Shiels, J.C., Callahan, J., Mehta, M.A. and Drobny, G.P. (1995) *Chem. Phys. Lett.*, **246**, 654–663.

Gregory, D.M., Mehta, M.A., Shiels, J.C. and Drobny, G.P. (1997) *J. Chem. Phys.*, **107**, 28–42.

Griffin, R.G. (1998) *Nat. Struct. Biol.*, **5**, 508–512.

Grigoriev, P., Schlegel, R., Dornberger, K. and Gräfe, U. (1995) *Biochim. Biophys. Acta*, **1237**, 1–5.
de Groot, H.J.M., Smith, S.O., Kolbert, A.C., Courtin, J.M.L., Winkel, C., Lugtenburg, J., Herzfeld, J. and Griffin, R.G. (1990) *J. Magn. Reson.*, **91**, 30–38.
Gullion, T. and Schaefer, J. (1989) *Adv. Magn. Reson.*, **13**, 57–83.
Harbison, G.S., Jelinski, L.W., Stark, R.E., Torchia, D.A., Herzfeld, J. and Griffin, R.G. (1984) *J. Magn. Reson.*, **60**, 79–82.
Hartzell, C.J., Pratum, T.K. and Drobny, G.P. (1987a) *J. Chem. Phys.*, **87**, 4324–4331.
Hartzell, C.J., Whitfield, M., Oas, T.G. and Drobny, G.P. (1987b) *J. Am. Chem. Soc.*, **109**, 5966–5969.
Heise, B., Leppert, J. and Ramachandran, R. (2000) *Solid State Nucl. Magn. Reson.*, **16**, 177–187.
Hing, A.W. and Schaefer, J. (1993) *Biochemistry* **32**, 7593–7604.
Hing, A.W., Vega, S. and Schaefer, J. (1992) *J. Magn. Reson.*, **96**, 205–209.
Hing, A.W., Vega, S. and Schaefer, J. (1993) *J. Magn. Reson.*, **103**, 151–162.
Hirsh, D.J., Hammer, J., Maloy, W.L., Bazyk, J. and Schaefer, J. (1996) *Biochemistry*, **35**, 12733–12741.
Hong, M., Gross, J.D. and Griffin, R.G. (1997a) *J. Phys. Chem.*, **101**, 5869–5874.
Hong, M., Gross, J.D., Rienstra, C.M., Griffin, R.G., Kumashiro, K.K. and Schmidt-Rohr, K. (1997b) *J. Magn. Reson.*, **129**, 85–92.
Hong, M., Gross, J.D., Hu, W. and Griffin, R.G. (1998) *J. Magn. Reson.*, **135**, 169–177.
Ishii, Y., Terao, T. and Kainosho, M. (1996) *Chem. Phys. Lett.*, **256**, 133–140.
Ketchem, R.R., Hu, W. and Cross, T.A. (1993) *Science*, **261**, 1457–1460.
Kovacs, F.A. and Cross, T.A. (1997) *Biophys. J.*, **73**, 2511–2517.
Li, Y., Krekel, F., Ramilo, C.A., Amrhein, N. and Evans, J.N.S. (1995) *FEBS Lett.*, **377**, 208–212.
Leppert, J., Heise, B. and Ramachandran, R. (1999) *J. Magn. Reson.*, **139**, 382–388.
Leppert, J., Heise, B. and Ramachandran, R. (2000a) *J. Magn. Reson.*, **145**, 307–314.
Leppert, J., Heise, B. and Ramachandran, R. (2000b) *J. Biomol. NMR*, **18**, 153–164.
Leppert, J., Heise, B. and Ramachandran, R. (2001) *Solid State NMR*, in press.
Linder, M., Höhener, A. and Ernst, R.R. (1980) *J. Chem. Phys.*, **73**, 4959–4970.
Marassi, F.M. and Opella, S.J. (1998) *Curr. Opin. Struct. Biol.*, **8**, 640–648.
Munowitz, M. and Griffin, R.G. (1982) *J. Chem. Phys*., **76**, 2848–2858.
Munowitz, M. and Griffin, R.G. (1983) *J. Chem. Phys*., **78**, 613–617.
North, C.L., Barranger-Mathys, M. and Cafiso, D.S. (1995) *Biophys. J.*, **69**, 2392–2397.
Oas, T.G., Hartzell, C.J., McMahon, T.J., Drobny, G.P. and Dahlquist, F.W. (1987) *J. Am. Chem. Soc.*, **109**, 5956–5962.
Opella, S.J. (1997) *Nat. Struct. Biol.*, **4**, 845–848.
Opella, S.J., Stewart, P.L. and Valentine, K.G. (1987) *Q. Rev. Biophys.*, **19**, 7–49.
Pang, Y., Wang, L., Pellecchia, M., Kurochkin, A.V. and Zuiderweg, E.R.P. (1999) *J. Biomol. NMR*, **14**, 197–306.
Pellechia, M., Pang, Y., Wang, L., Kurochkin, A.V., Kumar, A. and Zuiderweg, E.R.P. (1999) *J. Am. Chem. Soc.*, **121**, 9165–9170.
Reif, B., Diener, A., Henning, M., Maurer, M. and Griesinger, C. (2000) *J. Magn. Reson.*, **143**, 45–68.
Rhim, W.K., Elleman, D.D. and Vaughan, R.W. (1973) *J. Chem. Phys.*, **59**, 3740–3749.
Sanders II, C.R., Hare, B.J., Howard, K.P. and Prestegard, J.H. (1994) *Prog. NMR Spectrosc.*, **26**, 421–444.
Sansom, M.S.P. (1993a) *Q. Rev. Biophys.*, **26**, 365–421.
Sansom, M.S.P. (1993b) *Eur. Biophys. J.*, **22**, 105–124.
Schaefer, J. (1999) *J. Magn. Reson.*, **137**, 272–275.
Schmidt-Rohr, K. and Spiess, H.W. (1994) *Multidimensional Solid State NMR and Polymers*, Academic Press, London.
Shaw, W.J., Long, J.R., Dindot, J.L., Campbell, A.A., Stayton, P.S. and Drobny, G.P. (2000) *J. Am. Chem. Soc.*, **122**, 1709–1716.
Shoji, A., Ando, S., Kuroki, S., Ando, I. and Webb, G.A. (1993) *Annu. Rep. NMR Spectrosc.*, **26**, 55–98.
Smith, S.O., Aschheim, K. and Groesbeek, M. (1996) *Q. Rev. Biophys.*, **29**, 395–449.
Takeda, N., Kuroki, S., Kurosu, H. and Ando, I. (1999) *Biopolymers*, **50**, 61–69.
Takegoshi, K., Imaizumi, T. and Terao, T. (2000) *Solid State NMR*, **16**, 271–278.
Teng, Q. and Cross, T.A. (1989) *J. Magn. Reson.*, **85**, 439–447.
Teng, Q., Iqbal, M. and Cross, T.A. (1992) *J. Am. Chem. Soc.*, **114**, 5312–5321.
Ternovsky, V.I., Grigoriev, P.A., Berestovsky, G.N., Schlegel, R., Dornberger, K. and Gräfe (1997) *Membr. Cell Biol.*, **11**, 497–505.
Wishart, D.S., Bigam, C.G., Yao, J.,Abilgaard, F.,Dyson, H.J., Oldfield, E.,Markley, J.L. and Sykes, B.D. (1995) *J. Biomol. NMR*, **6**, 135–140.
Yang, D., Konrat, R. and Kay, L.E. (1997) *J. Am. Chem. Soc.*, **119**, 11938–11940.
Yang, D. and Kay, L.E. (1998) *J. Am. Chem. Soc.*, **120**, 9880–9887.